JACS
JOURNAL OF THE AMERICAN CHEMICAL SOCIETY
Article
pubs.acs.org/JACS

Kinetics and Thermodynamics of Chlorpromazine Interaction with Lipid Bilayers: Effect of Charge and Cholesterol

Patrícia T. Martins,[†] Adrian Velazquez-Campoy,[‡,§] Winchil L. C. Vaz,[†] Renato M. S. Cardoso,[†] Joana Valério,[∥] and Maria João Moreno*[,†]

[†]Chemistry Department FCTUC, Largo D. Dinis, Rua Larga, 3004-535 Coimbra, Portugal

[‡]Institute of Biocomputation and Physics of Complex Systems (BIFI), Universidad de Zaragoza, 50018 Zaragoza, Spain, Unidad Asociada BIFI-IQFR, CSIC, Zaragoza, Spain

[§]Fundación ARAID, Diputación General de Aragón, Spain

[∥]Instituto de Tecnologia Química e Biológica − UNL, Av. da República-EAN, 2780-157 Oeiras, Portugal

Supporting Information

ABSTRACT: Passive transport across cell membranes is the major route for the permeation of xenobiotics through tight endothelia such as the blood−brain barrier. The rate of passive permeation through lipid bilayers for a given drug is therefore a critical step in the prediction of its pharmacodynamics. We describe a detailed study on the kinetics and thermodynamics for the interaction of chlorpromazine (CPZ), an antipsychotic drug used in the treatment of schizophrenia, with neutral and negatively charged lipid bilayers. Isothermal titration calorimetry was used to study the partition and translocation of CPZ in lipid membranes composed of pure POPC, POPC:POPS (9:1), and POPC:Chol:POPS (6:3:1). The membrane charge due to the presence of POPS as well as the additional charge resulting from the introduction of CPZ in the membrane were taken into account, allowing the calculation of the intrinsic partition coefficients (K_P) and the enthalpy change (ΔH) associated with the process. The enthalpy change upon partition to all lipid bilayers studied is negative, but a significant entropy contribution was also observed for partition to the neutral membrane. Because of the positive charge of CPZ, the presence of negatively charged lipids in the bilayer increases both the observed amount of CPZ that partitions to the membrane (K_P^{obs}) and the magnitude of ΔH. However, when the electrostatic effects are discounted, the intrinsic partition coefficient was smaller, indicating that the hydrophobic contribution was less significant for the negatively charged membrane. The presence of cholesterol strongly decreases the affinity of CPZ for the bilayer in terms of both the amount of CPZ that associates with the membrane and the interaction enthalpy. A quantitative characterization of the rate of CPZ translocation through membranes composed of pure POPC and POPC:POPS (9:1) was also performed using an innovative methodology developed in this work based on the kinetics of the heat evolved due to the interaction of CPZ with the membranes.

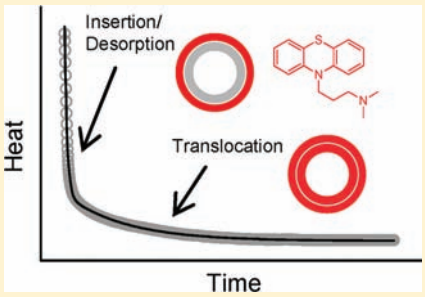

INTRODUCTION

Passive transport across cell membranes is the major route for the permeation of xenobiotics through tight epithelia, such as the vascular endothelium that constitutes the blood brain barrier. The rate of passive permeation through lipid bilayers, a critical step in the prediction of pharmacodynamics, is usually evaluated from the drug hydrophobicity with little consideration for the rate of insertion/desorption or translocation through the lipid bilayer. However, in most cases, the rate of the interaction (rather then the equilibrium partition) is the most relevant parameter,[1−3] and therefore it is very important to have kinetic details.

Chlorpromazine, a phenothiazine derived antipsychotic agent, is recommended in psychiatric disorders where neuroleptic sedative treatment is needed. It is amphiphilic and self-aggregates at a critical concentration, forming micelle-like structures, which undergo temperature- and concentration-dependent phase transitions.[4] Critical micelle concentrations (CMC) reported for chlorpromazine by different authors, using different techniques and experimental conditions, are scattered over a range of 2 orders of magnitude (from 10^{-5} to 10^{-3} M). It should be noted that chlorpromazine has a tertiary amine ($pK_a = 9.35$[5]), and therefore intermolecular interactions depend strongly on the solution pH and ionic strength.[6] At conditions similar to those used in this study (22 °C, 10 mM phosphate buffer at pH 7.3, with 140 mM NaCl), the CMC was found to be 2×10^{-4} M.[6] Aggregation of CPZ at concentrations well below its CMC is well supported by literature,[7,8] and the structure of a dimer has actually been proposed.[4] To guarantee that CPZ is predominantly in the monomeric form, its concentration in the aqueous solution at pH ≈ 7 must be maintained below 3×10^{-5} M.[9]

Received: October 21, 2011
Published: January 31, 2012

   dx.doi.org/10.1021/ja209917q | J. Am. Chem. Soc. 2012, 134, 4184−4195

The mechanism of action of chlorpromazine involves interaction with membrane proteins, but effects mediated by the lipid bilayer must also be considered. In fact, the binding affinity of CPZ for erythrocyte ghost was found to be the same as for neutral membranes, leading the authors to the conclusion that CPZ does not interact with proteins in the erythrocyte membrane.[10,11] Characterization of the interaction of CPZ with lipid bilayers as well as its effects on their properties is, therefore, highly relevant. The interaction of CPZ with lipid bilayers prepared from phosphatidyl cholines has been widely studied, and there is evidence for a location of the charged amine group in the phosphate region, while the tricyclic ring inserts in the lipid bilayer affecting mostly the properties of the carbonyl and first methylene groups of the lipid.[12] The ionization properties of CPZ are somewhat affected by insertion in the lipid bilayer with a decrease in the value of pK_a to 8.3 in phosphocholine (lecithin) from egg yolk (egg PC) with or without cholesterol.[13] A more interfacial location of CPZ has been argued for the case of negatively charged membranes based on a larger area expansion of lipid monolayers upon interaction with CPZ.[14] The effect of CPZ on the properties of lipid bilayers has also been a subject of intense research. At very high CPZ concentrations, well above its CMC, the membrane is completely dissolved due to the formation of mixed micelles, while at lower concentrations membrane leakage and loss of lipid asymmetry is increased.[15−17] A depression in the main transition temperature of PC membranes is also observed at local CPZ concentrations above 5 mol %.[9,18] Induction of phase separation and domain morphology changes have been reported for membranes prepared from mixtures of neutral and negative lipids,[18−20] and stabilization of phosphoethanolamine (PE) lamellar phases has also been shown.[21] Suppression of multi drug resistance by CPZ has been reported in the literature for some time,[22] and this has received special attention recently.[23,24] However, the details and mechanism of this important effect of CPZ in biomembranes are not known. The interpretation of the different effects of CPZ in lipid membranes is very difficult because its local concentration is usually not explicitly considered and most of the times is impossible to calculate because the partition coefficient at the conditions of the experiments is not known.

The partition coefficient of CPZ between the aqueous medium and lecithin bilayers has been accurately measured by Kitamura and co-workers[11,25−27] and others.[9,10] A decrease in the partition coefficient with the total concentration of CPZ, from 5 to 100 μM, was observed. At a total concentration of 10 μM and pH $\approx$ 7, the reported values for the partition coefficient of CPZ between water and egg PC are 9.9×10^3 [10] and 6.8×10^3,[25] being 5.4×10^3 for association with 1,2-dimyristoylphosphocholine (DMPC).[9] The value of pH was shown to affect significantly the affinity to the lipid bilayer that increases at higher values of pH,[10] indicating a higher partition coefficient for the neutral form. No quantitative interpretation was given for the dependence of the partition coefficient on CPZ concentration, although aggregation of CPZ in the aqueous phase was evoked. In this work, we will readdress this question taking into account the charge imposed in the bilayer by the cationic CPZ according to the Gouy−Chapman theory as was done previously for sodium dodecyl sulfate.[28,29] The introduction of cholesterol in the membrane was shown to decrease the partition coefficient of CPZ,[9,26] while the addition of negatively charged lipids increases the affinity of CPZ for the membrane.[30] We will characterize the effect of cholesterol and negative charge in the lipid bilayer in an attempt to give a quantitative interpretation to the variations observed.

The methodology used in the characterization of CPZ interaction with membranes is mostly based on changes in the second derivative of CPZ absorption in the UV,[10,25−27,30] but physical separation of the aqueous and membrane phases has also been used.[9] In this work, we use isothermal titration calorimetry (ITC), a very powerful technique that allows the measurement of the partition coefficient as well as the thermodynamic parameters for the interaction. The ITC technique has been generally used with high concentrations of ligands, and under those conditions saturation of the membrane may occur for the case of ligands with a high partition coefficient. Additionally, those high concentrations are not appropriate for ligands with a tendency to aggregate in the aqueous phase. We have recently shown that with the high sensitivity of modern ITC equipment, the ligand concentration may be reduced to levels previously accessible only by spectroscopic techniques,[28] allowing the direct characterization of partition to unperturbed membranes. Additionally, protocols have been recently developed that allow the qualitative evaluation of the kinetics of ligand translocation across the bilayers.[31−33] This parameter is of fundamental importance in the quantitative characterization of the association of ligands with lipid bilayers because it is necessary to know the amount of membrane phase that is accessible to the ligand (only the outer monolayer or both) and also because this is usually considered the rate-limiting step in their permeation through membranes.[34] In this work, we introduce new approaches that allow the quantitative measurement of the translocation rate constant using ITC.

We report here the kinetics and thermodynamics of the interaction of CPZ with large unilamelar vesicles (LUVs) prepared from pure POPC, POPC:POPS (9:1), and POPC:Chol:POPS (6:3:1) using isothermal titration calorimetry. The effect of CPZ concentration on the partition coefficient observed is quantitatively interpreted in terms of the charge imposed by CPZ in the membrane using the Gouy−Chapman theory. The relative rate of the insertion/desorption and translocation processes was obtained using the uptake and release protocols.[31] A quantitative evaluation of the translocation rate is also performed, for the case of the membranes in the liquid disordered phase studied, following an innovative methodology based on the kinetics of the heat evolved upon association of CPZ with the membranes. The equilibration of aqueous CPZ with the outer monolayer of LUVs occurs faster than the time resolution of the ITC, but a much slower process is observed due to translocation of CPZ into the inner monolayer of LUVs, which leads to the association of additional CPZ with the outer monolayer. The mathematical model to describe this biphasic heat variation was developed, and the rate constant of translocation was obtained as a function of both temperature and pH.

MATERIALS AND METHODS

Materials. 1-Palmitoyl-2-oleoyl-*sn*-glycero-3-phosphocoline (POPC), 1-palmitoyl-2-oleoyl-*sn*-glycero-3-phosphoserine (POPS), and cholesterol (Chol) were obtained from Avanti Polar Lipids (Alabaster, AL). Chlorpromazine (CPZ) and all other reagents and solvents were of high purity purchased from Sigma-Aldrich Química (Sintra, Portugal).

Preparation of Large Unilamellar Vesicles. Aqueous suspensions of lipids were prepared by evaporating a solution of the desired lipid or premixed lipid mixture in the azeotropic mixture of chloroform:methanol (87:13, v/v) by blowing dry nitrogen over the heated (blowing hot air over the external surface of the tube) solution and then leaving the residue in a vacuum desiccator for at least 8 h at room temperature. The solvent-free residue was hydrated with Hepes buffer (10 mM, pH 7.4) with 0.15 M NaCl, 1 mM EDTA, and 0.02% (m/v) NaN3 (hereafter termed buffer). The hydrated lipid was subjected to several cycles of gentle vortex/incubation for at least 1 h, to produce a suspension of multilamelar vesicles, that was then extruded in a water-jacketed extruder (Lipex Biomembranes, Vancouver, British Columbia, Canada) using a minimum of 10 passes, through two stacked polycarbonate filters (Nucleopore) with a pore diameter of 0.1 μm.[35] The hydration and extrusion steps were performed at room temperature for the case of POPC and POPC:POPS 9:1 and at 50 °C for membranes prepared from POPC:Chol:POPS 6:3:1. The same procedure was followed for vesicles containing CPZ, except that an appropriate volume a stock solution of CPZ 5 mM in chloroform:methanol (87:13, v/v) was added to the lipids and thoroughly mixed prior to vesicle preparation.

The final phospholipid concentrations in the LUVs were determined using a modified version of the Bartlett phosphate assay,[36] and the final cholesterol concentration was determined by the Lieberman−Burchard method as described by Taylor et al.[37] CPZ concentrations were determined by their absorbance at 310 nm using an extinction coefficient of 3260 M^{-1} cm^{-1} in aqueous solution.

Characterization of the LUVs. The average size of the LUVs at 25 °C and their zeta potential were measured on a Malvern Nano ZS (Malvern Instruments, Malvern, UK). The measurements of LUV size were performed at a total lipid concentration of 1 mM using samples extruded at 1−10 mM through 100 nm pore size filters. Ten independent samples were characterized for POPC LUVs. The samples were monodisperse with an average diameter from 96 to 117 nm, when evaluated from the size distribution by volume, leading to an average diameter of 106 ± 7 nm. Some samples were also characterized for the other lipid compositions used in this work, and the average diameter obtained was 101 nm for POPC:POPS 9:1 LUVs and 117 nm for POPC:Chol:POPS 6:3:1.

The mobility of the LUVs containing 10% POPS was also measured, and the ζ potential was calculated,[38] using the viscosity[39] and dielectric constant[40] at the concentration of NaCl present in solution, with $\zeta = -17 \pm 1$ mV for POPC:POPS 9:1 and $\zeta = -24 \pm 1$ mV for POPC:Chol:POPS 6:3:1 in the aqueous buffer (10 mM Hepes buffer at pH 7.4 with 0.15 M NaCl, 1 mM EDTA, and 0.02% (m/v) NaN3). The value of the ζ potential of LUVs containing CPZ at concentrations from 2 to 10 molar % was also measured for the lipid compositions POPC and POPC:POPS 9:1 at a total lipid concentration of 2 and 4 mM, respectively. For some compositions, ζ was too small to be accurately measured at the ionic strength used in this work, and it was measured in aqueous buffer at the same pH but with different concentrations of NaCl. For those compositions, ζ at 150 mM NaCl was calculated from the results obtained at smaller ionic strengths, assuming the same dependence as observed for the mixtures at which it could be measured at all ionic strengths.

Multilamellarity in the LUVs was evaluated from the relative weight of the different steps in the reduction of NBD-C_{16} or NBD-DMPE, at a molar concentration of 0.1%, by dithionite added to the aqueous solution outside the LUVs.[41,42] Typical results are shown in the Supporting Information. The fraction of lipid in inner bilayers obtained by both methods was similar, being 9 ± 2% for LUVs with the lipid composition POPC:Chol:POPS 6:3:1, 12 ± 4% for POPC:POPS 9:1, and 18 ± 5% for POPC LUVs.

Isothermal Titration Calorimetry. Titrations were performed on a VP-ITC instrument from MicroCal (Northampton, MA) with a reaction cell volume of 1410.9 μL, at 25 and 37 °C. The injection speed was 0.5 μL s^{-1}, stirring speed was 459 rpm, and the reference power was 10 μcal s^{-1}. As recommended by the manufacturer, a first injection of 4 μL was performed before the experiment was considered to start, to account for diffusion from/into the syringe during the equilibration period, but the injected amount was taken into consideration in the calculations. The titration proceeded with additions of 10 μL per injection. Amphiphilic ligands like CPZ may adsorb to some equipment parts, in particular to the filling syringe, reducing the amount of ligand available. To overcome this difficulty, after cleaning thoroughly with water, the equipment cell was rinsed with a solution with the same composition as the solution to be used in the experiment before filling with the required titration solution. All solutions were previously degassed for 15 min.

Two protocols for the ITC experiments were used in this work: (i) uptake, in which liposomes were injected into a CPZ solution in the cell, and (ii) release, in which a liposome solution containing CPZ was injected into the cell containing buffer. The purpose of the uptake and release protocols was to obtain thermodynamic parameters for the reaction as well as a qualitative evaluation of the translocation rate constant.[31,33]

The thermograms were integrated using the data analysis software Origin 7.0 as modified by MicroCal to deal with ITC experiments, and the resulting differential titration curves were fitted with the appropriate equations using Microsoft Excel and the Add-In Solver. The concentrations in the cell were calculated taking into account the volume that overflows the cell due to the addition of solution from the syringe considering that overflow is faster than mixing, meaning that the composition of the solution leaving the cell is the equilibrium composition before the addition.[43−45]

Partition Model. The predicted heat evolved in titration step i, $q(i)$, is calculated by eq 1, and the best fit of the model to the experimental values was obtained through minimization of the square deviations between the experimental and the predicted heat per injection for all of the titration steps, as described previously:[28]

$$q(i) = \Delta H\left(n_{\mathrm{CPZ\_L}}(i) - n_{\mathrm{CPZ\_L}}(i-1)\left(1 - \frac{V(i)}{V_{\mathrm{cell}}}\right)\right) + q_{\mathrm{dil}} \quad (1)$$

where $V(i)$ is the injection volume, V_{cell} is the volume of the calorimetric cell, and q_{dil} is the "heat of dilution" (residual heat due to nonbinding phenomena). The amount of CPZ associated with the lipid bilayer is calculated assuming simple partition between the aqueous and the lipid phase, kinetic scheme I.

Kinetic Scheme I − Interaction of CPZ with the liposomes considered as a lipid phase:

$$\mathrm{CPZ_W} \overset{K_P^{\mathrm{obs}}}{\longleftrightarrow} \mathrm{CPZ_L}$$

The observed partition coefficient (K_P^{obs}) is given by the ratio of the concentrations of CPZ in each phase, calculated with respect to the volume of the respective phase, and is given by the upper line of eq 2, where $n_{\mathrm{CPZ\_T}}$ is the total number of moles of CPZ of which $n_{\mathrm{CPZ\_W}}$ are in the aqueous and $n_{\mathrm{CPZ\_L}}$ are in the lipid phase.

$$K_P^{\mathrm{obs}} = \frac{n_{\mathrm{CPZ\_L}}/V_L}{n_{\mathrm{CPZ\_W}}/V_W} = \frac{n_{\mathrm{CPZ\_L}}/([L]\bar{V}_L V_T)}{n_{\mathrm{CPZ\_W}}/V_T}$$

$$n_{\mathrm{CPZ\_L}} = n_{\mathrm{CPZ\_T}}\frac{K_P^{\mathrm{obs}}[L]\bar{V}_L}{1 + K_P^{\mathrm{obs}}[L]\bar{V}_L} \quad (2)$$

In the equation, V_T is the total volume, and V_L and V_W are the volumes of the lipid and aqueous phases, respectively. The molar volumes, $\bar{V}_L$, considered for the lipids used in this work were 0.795 dm^3 mol^{-1} for POPC[46] and POPS and 0.325 dm^3 mol^{-1} for cholesterol.[47]

Values of the adjustable parameters, K_P^{obs} and ΔH, are generated by the Microsoft Excel Add-In Solver, and the corresponding heat evolved at each injection is calculated using eq 1 and the lower line of eq 2. This is compared to the experimental values obtained in the titration, and the square difference is minimized.

Depending on the relative rates of translocation and insertion/desorption, CPZ may or may not be equally distributed between the two bilayer leaflets. This requires the substitution of CPZ

concentration by its effective concentration, [CPZ]*, which depends on the effective lipid concentration, [L]*, according to eq 3. This introduces the equilibration factor, γ, which is a measure of the fraction of lipid accessible to CPZ during the titration experiment, with values of 1 for fully permeable (fast translocation of ligand) and 0.5 for impermeable membranes (slow translocation of ligand).

For experiments following the uptake protocol (addition of lipid to ligand in the aqueous phase), all ligand is accessible for partition, and the effective lipid concentration is either equal to its total concentration (case of fast translocation) or is reduced to the lipid in the outer monolayer (case of slow translocation), according to eq 3. In this type of experiments, if γ is unknown, the uncertainty is propagated to the partition coefficient, but the calculated enthalpy variation is accurate. On the other hand, in experiments following the release protocol, both the lipid effective concentration and the available moles of ligand must be calculated from eq 3. In this situation, both K_P and ΔH are affected by the uncertainty in γ. The combination of both protocols allows the calculation of the equilibration factor and, therefore, the accurate measurement of K_P and ΔH and a qualitative estimation of the translocation rate constant.

$$[L]^*(i) = [L]^*(i-1)\left\{1 - \frac{V(i)}{V_{cell}}\right\} + \gamma\left\{[L]^{Syr}\frac{V(i)}{V_{cell}}\right\}$$

$$n^*_{CPZ\_T}(i) = n^*_{CPZ\_T}(i-1)\left\{1 - \frac{V(i)}{V_{cell}}\right\} + \{\gamma[CPZ]^{Syr}_L + [CPZ]^{Syr}_W\}V(i) \quad (3)$$

where the index i refers to the injection number, the superscript Syr indicates concentrations in the syringe, and the subscripts L and W indicate the phase where CPZ is dissolved, being L for the lipid and W for water (T for the sum of both).

Correction for the Electrostatic Effect. The partition coefficient obtained directly from the ratio of the concentrations in both phases, K_P^{obs}, is dependent on the total concentration of ligand in the bilayer due to the charge introduced by it and is related to the intrinsic partition coefficient (for an uncharged bilayer, K_P) via the electrostatic potential at the bilayer surface, Ψ_0, as described previously[28,29,48] and shown in eq 4. The bilayer charge density, σ, is related to the electrostatic potential at the bilayer surface, Ψ_0 (eq 5, first line), and may be calculated from the surface density of charged molecules in the bilayer (eq 5, second line). The difference between the values of σ calculated from both approaches is minimized by changing the values of the surface potential and intrinsic partition coefficient, allowing the computation of the best value for those two parameters.

$$K_P^{obs} = K_P e^{-zF\Psi_0/RT} \quad (4)$$

$$\sigma = \frac{\Psi_0}{|\Psi_0|}\sqrt{2000\varepsilon RT\sum_i C_i(e^{-z_iF\Psi_0/RT} - 1)}$$

$$\sigma = e_0\frac{\sum z_i(n_i/n_L)}{\sum A_j(n_j/n_L)} \quad (5)$$

where ε is the dielectric constant, R is the ideal gas constant, F is the Faraday constant, C_i is the concentration of the charged species i, with the charge z_i, e_0 is the elemental electrostatic charge, A_j is the area of the j component of the lipid bilayer (being 68 Å^2 for POPC and POPS,[29] 25 Å^2 for Chol,[49] and 39 Å^2 for CPZ[14]), n_j (n_i) is the number of moles of the membrane component j (i), and n_L is the number of moles of lipid. The charge considered for POPS was −1, and that of CPZ inserted in lipid bilayers at pH = 7.4 was +0.89 (considering its pK_a = 8.3[13]).

RESULTS AND DISCUSSION

Effect of Ligand Concentration. To obtain the partition of small molecules into lipid bilayers, the usual protocol is to titrate the ligand with increasing amounts of lipid.[28,32,50] One important factor is the eventual effects of ligand in the membrane,[28,51] and this was evaluated through the dependence of the observed partition coefficient on the total CPZ concentration when titrated with 5 mM POPC, assembled as 100 nm LUVs, at 25 °C. Given the positive charge on CPZ at the pH used (pH 7.4), a small rate of translocation is anticipated, and therefore the accessibility factor was assumed to be 0.5. The results obtained are shown in Figures 1 and 2.

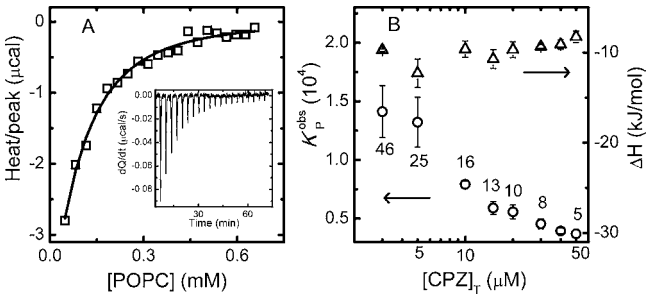

Figure 1. Titration of CPZ at different total concentrations with 5 mM POPC at 25 °C. Plot A: Typical titration curve obtained for $[CPZ]_T$ = 5 μM. The line is the best fit obtained with eqs 1 and 2. Plot B: Observed partition coefficients (K_P^{obs}, ○) and molar enthalpy change (ΔH, △) obtained by the best fit of eqs 1 and 2 to the experimental results. The numbers indicated are the ratio of lipid molecules per bound CPZ after the first 10 μL injection.

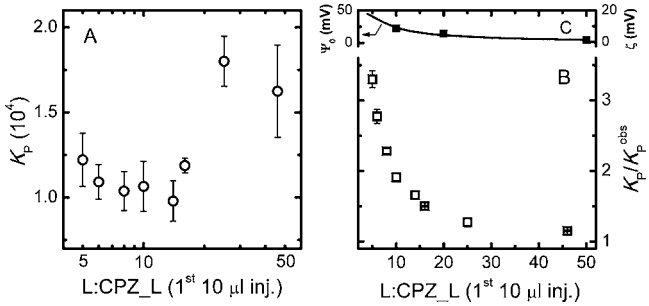

Figure 2. Effect of CPZ concentration on its partition to POPC bilayers at pH = 7.4 and 25 °C. Plot A: Intrinsic partition coefficients (K_P, ○) obtained for titration of CPZ at different total concentrations in the aqueous phase, between 2.5 and 50 μM, with POPC 5 mM. The results are indicated as a function of the lipid to bound CPZ ratio after the first 10 μL injection. Ideal conditions correspond to high values in this parameter, while they corresponded to low ligand concentrations in Figure 1. Plot B: Ratio between the values of the intrinsic and observed partition coefficient as a function of the local concentration of CPZ in the POPC bilayer. Plot C: Surface potential predicted by the Gouy−Chapman theory (Ψ_0), eqs 2−5, and the measured zeta potential (ζ) at the indicated ratios of POPC to CPZ.

Figure 1, plot A, shows a typical titration of CPZ at a total concentration of 5 μM. The interaction parameters, obtained with eqs 1 and 2, are represented in Figure 1, plot B, together with the parameters obtained for all of the concentrations of CPZ studied. The numbers indicated in plot B are the ratio of lipid per bound CPZ after the first 10 μL injection. This ratio increases as the titration proceeds due to the increase in the lipid concentration.

The observed partition coefficient (K_P^{obs}) is independent of local concentration of CPZ for very small molar fractions of ligand (smaller than 4%, that is, over 25 lipid molecules per bound CPZ). For larger local concentrations of CPZ, the observed partition coefficient shows a significant decrease.

dx.doi.org/10.1021/ja209917q | J. Am. Chem. Soc. 2012, 134, 4184−4195

This result was expected due to the positive charge imposed by CPZ in the bilayer, and it may be accounted for using eqs 4 and 5 from which the intrinsic partition coefficient K_P may be obtained (Figure 2, plot A).

Some dependence of K_P on the local concentration of CPZ is still observed, although it is much smaller than that observed for K_P^{obs}, reflecting deviations from ideal behavior. The small increase in K_P observed for very small and very large local concentrations of CPZ may reflect an overestimation of the membrane surface potential by the Gouy−Chapman theory due to the limitations of this approach, which does not consider the discreteness-of-charge.[48,52−55] Additionally, the binding of sodium and chloride to POPC was not taken into account. This is not expected to influence significantly the results due to the small binding constants reported for the binding of those ions to phosphocoline membranes and the similar affinities of both ions.[56] The abrupt variation of K_P between 1:25 and 1:10 CPZ:lipid molecules possibly indicates a distinct mode of interaction between CPZ and the POPC bilayer, which may be related to the formation of aggregates in the membrane. In fact, significant effects of CPZ in the properties of membranes have been observed at comparable CPZ concentrations.[9,15−18]

The ratio between the observed and the intrinsic partition coefficient is represented in Figure 2, plot B, and it may be seen that the two parameters converge for low local concentrations of CPZ (less than 4% molar ratio), giving $K_P = (1.7 \pm 0.2) \times 10^4$ with $\Delta H = -12 \pm 2$ kJ mol^{-1} and $K_P^{obs} = (1.5 \pm 0.4) \times 10^4$ with $\Delta H = -13 \pm 1$ kJ mol^{-1} at 25 °C. The parameters obtained are very similar to those reported in the literature for partition of CPZ to EggPC SUVs using small ligand concentrations where the partition was followed through the variations in CPZ absorption spectra (K_P^{obs} =1.5 × 10^4 at 37 °C,[10] with a van't Hoff enthalpy of −9.5 kJ mol^{-1} [27]).

When the local concentration of CPZ is high, the calculation of the intrinsic partition coefficient is strongly dependent on the electrostatic model used. To have some indication on the adequacy of eqs 4 and 5, we have measured the ζ potential of POPC LUVs loaded with CPZ at a ligand to lipid molar ratio of 1:50, 1:20, and 1:10. The dependence of ζ on the local concentration of CPZ is similar to that of the surface potential predicted from the Gouy−Chapman theory, but the magnitude of the ζ potential is significantly smaller, Figure 2, plot C. Some difference was anticipated because ζ is the potential at the hydrodynamic shear plane and not at the bilayer surface, which is the potential predicted by the equations used in this work and felt by CPZ when inserted in the bilayer.[38]

Given the difficulties in the correction for the electrostatic effects, the uncertainty associated with the parameters required, and the higher complexity in data analysis, it is therefore preferable to use the lowest concentration of ligand that generates a good signal-to-noise ratio (5 μM) and analyze the results in terms of the partition coefficient directly obtained experimentally, K_P^{obs}. A total concentration of CPZ corresponding to a lipid to CPZ bound ratio of at least 25, in the first 10 μL injection, was used throughout the rest of the work.

At the pH used in the experiments, 99% of CPZ is in the protonated state (pK_a = 9.35[5]), and based on the reported value of the ionization constant for CPZ inserted in lipid bilayers (pK_a = 8.3[13]), 89% remains in the charged protonated state after interaction with the membranes. Because of the importance of this process in the interpretation of the interaction enthalpies obtained, we have performed titrations in buffers with different ionization enthalpies to evaluate the fraction of protons released upon partition to the POPC bilayers.[57] No significant dependence of ΔH on the ionization enthalpy of the buffer was observed, an indication that the fraction of protons released or bound upon association with the membrane is ≤0.1 (results not shown).

Translocation of CPZ in Membranes Prepared with POPC. In the previous section, we have considered that CPZ translocation was slower than the characteristic time for the titration; this assumption was required for the preliminary experiments to identify the most appropriate ligand and lipid concentrations. The rate of translocation will now be evaluated, using the selected best CPZ and lipid concentrations, and this will be first attempted through the global best fit of titrations performed according to the uptake and release protocols.[31]

ITC uptake and release curves obtained at 25 °C for CPZ titration with POPC LUVs are represented in Figure 3. The uptake experiment was performed injecting aliquots of 5 mM POPC into 5 μM CPZ in buffer, while in the release experiment aliquots of 15 mM POPC preloaded with 0.15 mM CPZ (POPC:CPZ molar ratio equal to 100) were injected into the sample cell containing buffer, both spaced by 200 s between injections.

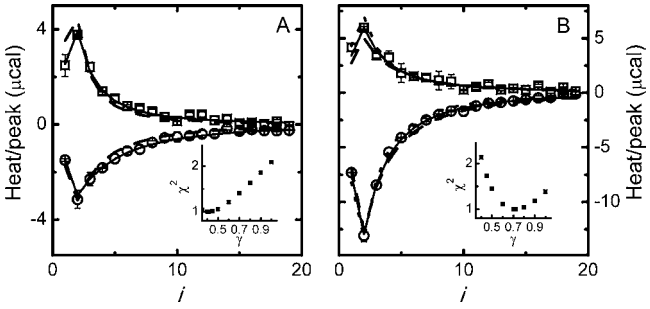

Figure 3. Titrations curves obtained for the uptake (○) and release (□) protocols with POPC membranes. Plot A: Experiments at 25 °C. The lines are the best fit using γ = 0.5 (continuous line) and γ = 1 (dashed line). Plot B: Experiments at 37 °C. The lines are the best fit obtained with γ = 0.5 (− − −), γ = 1 (- - -), and γ = 0.7 (−). The insets show the dependence of the square deviation between the global best fit and the experimental results (χ^2) as a function of γ.

The experiment performed at 25 °C was well fitted by eqs 1−5, using a lipid accessibility factor of γ = 0.5 in eq 3, and the average thermodynamic parameters found previously for titrations of CPZ at 5 μM using the uptake protocol. In contrast, if an accessibility factor of 1 was imposed, the best global fit of the uptake and release experiments was not acceptable (Figure 3, plot A). The variation of the global fit χ^2 on the accessibility factor is shown in the inset with a minimum for γ = 0.4−0.5 and increasing sharply for $\gamma \geq 0.55$. This indicates that translocation of CPZ between the two bilayer leaflets is negligible during the time scale of the experiment at 25 °C. Those results show, additionally, that the fraction of lipid exposed to the aqueous media outside the LUVs is between 40% and 50% and, conversely, that the fraction of lipid present in inner bilayers is smaller than 20%. This is in agreement with the results obtained by other methods for the multilamellarity of the LUVs used in this work (see the Supporting Information for details).

The results obtained in the experiments at 37 °C are shown in Figure 3B. In this case, the best global fit for the uptake and release experiments leads to $\gamma \approx 0.7$, and a good fit could not be

dx.doi.org/10.1021/ja209917q | J. Am. Chem. Soc. 2012, 134, 4184−4195

obtained in any of the two thermodynamically meaningful cases (γ = 0.5 or 1); see inset in the figure. Intermediate values of accessibility factors reflect translocation rates comparable to the titration experiment, but a quantitative characterization of this parameter cannot be performed using this approach.[48]

In an attempt to separate the processes of equilibration of CPZ between the outer monolayer and the aqueous phase and its translocation across the bilayer, the time between injections was increased from 200 to 3600 s in an uptake experiment. The results obtained are shown in Figure 4 where it can be seen that

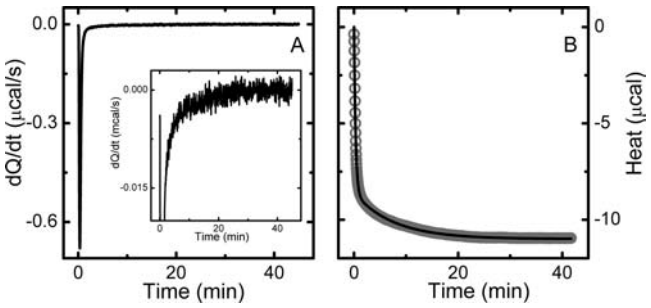

Figure 4. Kinetic profile of the heat evolved due to the addition of POPC vesicles to an aqueous CPZ solution. Plot A: Injection of 10 μL of POPC 15 mM into CPZ 15 μM, at 37 °C, recorded for 3600 s (evidence for the slower step). Plot B: Cumulative heat in time for the partition of CPZ into POPC LUVs. The line is the best fit of eq 6 with the rate constants 3.1×10^{-2} and 1.3×10^{-3} s^{-1} for the fast and slow process, respectively.

most heat is evolved during the first minutes with an additional slower step being also present that extends up to 40 min (see inset of plot A). The fast process corresponds to the partition of CPZ into the outer monolayer of LUVs, and the slower step was attributed to the entry of new CPZ into the outer monolayer due to translocation of CPZ from the outer into the inner monolayer. It should be noted that translocation in itself does not originate any heat change because both initial and final states are energetically equivalent. However, as CPZ leaves the outer monolayer, due to translocation into the inner, some additional CPZ partitions between the aqueous phase and the outer monolayer of the LUVs, according to kinetic scheme II and eq 6.

Kinetic Scheme II − Interaction of CPZ with the outer (o) and inner (i) leaflets of LUVs:

$$\mathrm{CPZ_W} \underset{k_-}{\overset{k_+[\mathrm{LUV}]}{\rightleftharpoons}} \mathrm{CPZ_L^o} \overset{k_f}{\leftrightarrow} \mathrm{CPZ_L^i}$$

$$\frac{d[\mathrm{CPZ}]_W}{dt} = k_-[\mathrm{CPZ}]_L^o - k_+[\mathrm{LUV}][\mathrm{CPZ}]_W$$

$$\frac{d[\mathrm{CPZ}]_L^o}{dt} = k_+[\mathrm{LUV}][\mathrm{CPZ}]_W - k_-[\mathrm{CPZ}]_L^o + k_f([\mathrm{CPZ}]_L^i - [\mathrm{CPZ}]_L^o)$$

$$\frac{d[\mathrm{CPZ}]_L^i}{dt} = k_f([\mathrm{CPZ}]_L^o - [\mathrm{CPZ}]_L^i) \quad (6)$$

where k_+, k_-, and k_f are the rate constants for insertion into, desorption from, and translocation through the lipid bilayer. The heat evolved at a given time after each injection is proportional to the variation in the total amount of CPZ in the membrane (in the outer plus inner leaflets), and the rate constants may be obtained from the best fit of eq 6 to the experimental curve. As is evident in Figure 4A, the fast step dominates the variation of the differential heat, and this decreases the statistical weight of the best fit to the most relevant slower process. The weights of the two processes become comparable when the cumulative heat is represented, Figure 4B, and we have therefore opted for performing the best fit of the cumulative heat with the numerical integration of eq 6. The results presented were obtained after the injection of 10 μL of a 15 mM POPC suspension into CPZ at 15 μM (a small concentration of POPC was already in the cell due to the injection of the recommended 4 μL), and the weight of the two steps leads to a 20% increase of CPZ in the membrane due to partitioning to the lipid in the inner leaflet, in agreement with that predicted from the value of the partition coefficient obtained using standard protocols (see Table 1).

The rate constants obtained from the best fit of eq 6 to the cumulative heat shown in Figure 4B were 3.1×10^{-2} and 1.3×10^{-3} s^{-1} for the fast and slow processes, respectively. The fast process is due to partitioning to the outer monolayer (k_+[LUV] + k_-), but the characteristic rate constant obtained cannot be used to calculate the rate of insertion and desorption because the heat variation is being limited by the time response of the equipment (~10 s). To improve the confidence in the nature of the process generating the slower heat variation, we have performed the experiment at different values of pH from 6.5 to 8.0. The reported pK_a of CPZ inserted in lipid bilayers is equal to 8.3,[13] from which the fraction of ligand in the neutral form at the different values of pH may be calculated to be 0.016 at pH = 6.5, 0.05 at pH = 7, 0.11 at pH = 7.4, and 0.33 at pH = 8. This increase in the fraction of neutral form with pH is expected to accelerate significantly the rate of translocation (eq 7), and

Table 1. Kinetic and Thermodynamic Parameters for CPZ Translocation in POPC and POPC:POPS 9:1 LUVs and Parameters Obtained for CPZ Partition into Those Membranes Taking into Account Partial Translocation during the Titration

		translocation			partition		
	T (°C)	k_f^a (10^{-4} s^{-1})	ΔH (kJ mol^{-1})	$T\Delta S^{(37\ °C)}$ (kJ mol^{-1})	K_p^{obs} (10^4)	ΔH (kJ mol^{-1})	$T\Delta S$ (kJ mol^{-1})
POPC	25	3.9[b]	62 ± 12	−32 ± 8	1.2 ± 0.4	−12 ± 1	12
	37	10 ± 2			1.0 ± 0.3	−11 ± 1	13
POPC:POPS (9:1)	25	6.6 ± 0.7	49 ± 10	−44 ± 7	1.4 ± 0.2	−21 ± 3	3
	37	15 ± 1			1.3 ± 0.1	−22 ± 3	2

[a]The average values shown are from the best fit shown in Figure 6, and the standard deviations were calculated from the three experimental measurements performed at the indicated temperature. [b]Extrapolated from the results obtained between 30 and 40 °C, Figure 7.

dx.doi.org/10.1021/ja209917q | J. Am. Chem. Soc. 2012, 134, 4184−4195

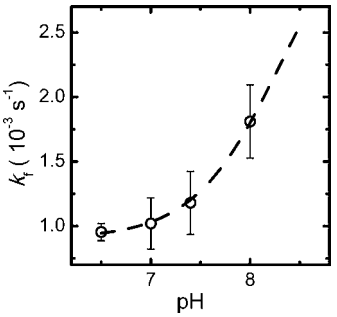

Figure 5. Translocation rate constants obtained for CPZ in POPC lipid bilayers at different pH buffer solutions. The line is the best fit for the global theoretical translocation rate constant of CPZ, with pK_a = 8.3 and k_f for the neutral and cationic forms equal to 3.6×10^{-3} and 9.0×10^{-4} s^{-1}, respectively.

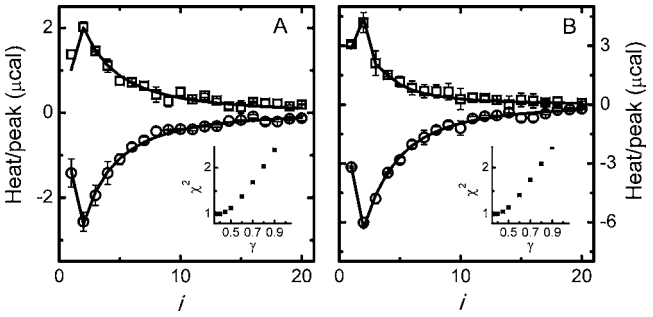

Figure 6. Uptake (○) and release (□) experiments with membranes composed of POPC:Chol:POPS (6:3:1) at (A) 25 °C and (B) at 37 °C. The lines are the best fit of eqs 1−6 with γ = 0.5, and K_P = 5.8×10^3, ΔH = −4 kJ mol^{-1} at 25 °C and K_P = 4.1×10^3, ΔH = −12 kJ mol^{-1} at 37 °C. Insets are as in Figure 3.

this was in fact observed (Figure 5). The global rate of translocation is given by:

$$k_f = k_f^+[CPZ^+] + k_f^0[CPZ^0] \quad (7)$$

where $[CPZ^+]$ and $[CPZ^0]$ are the concentrations of CPZ in its cationic and neutral states, respectively, and k_f^+ and k_f^0 are their respective translocation rate constants. The concentrations of neutral and charged CPZ species are calculated from its ionization constant (K_a) and solution pH (eq 8).

$$[CPZ^0] = \frac{[CPZ]_T K_a}{10^{-pH} + K_a}; \; [CPZ^+] = [CPZ]_T - [CPZ^0] \quad (8)$$

From the dependence of the rate of translocation with the value of pH, one can obtain the rate constant for translocation of the neutral form, k_f^0, as well as that of the cationic form, k_f^+, being 3.6×10^{-3} and 9.0×10^{-4} s^{-1}, respectively, at 37 °C. The excellent fit of the predicted dependence with pH to the observed variation gives support to the interpretation that this slow step is due to translocation of CPZ between the bilayer leaflets. The ratio between the rate constants for translocation of the neutral and charged form is equal to 4. This is smaller than anticipated based on the usually observed much faster permeation of neutral ligands as compared to charged ones.[58−60] However, it should be noted that for most solutes, when the Meyer−Overton rule applies,[34] the rate of permeation is directly proportional to both the translocation rate and the fraction of solute associated with the outer monolayer (which is given by the partition coefficient), and, in fact, for the few ligands where the two processes have been measured, the ratio between the rates of translocation of neutral and charged species may be even smaller than the one obtained for CPZ ($k_f^0/k_f^- = 2$ for an aromatic carboxylic acid[58]). Additionally, the translocation rate constant obtained for the neutral form is strongly dependent on the value considered for the ionization constant (e.g., if pK_a = 8.5 is assumed, the value obtained from the best fit is $k_f^+ = 4.6 \times 10^{-3}$ s^{-1}, leading to a ratio equal to 5).

The experiment at pH = 7.4 was performed at different temperatures, from 30 to 40 °C, to obtain the thermodynamic parameters of the translocation step. The results are shown in the next section (Figure 7) together with data for POPC:POPS mixtures.

Translocation of CPZ in Membranes Containing POPS. The combination of uptake and release protocol was successfully used to obtain qualitative information on the

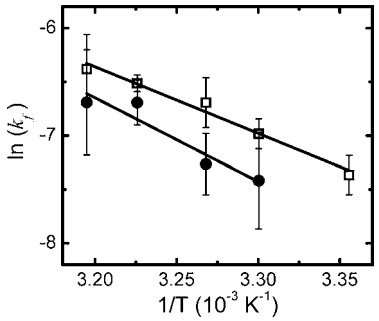

Figure 7. Translocation rate constant for chlorpromazine in membranes prepared from pure POPC (●) and POPC:POPS (9:1) (□). The lines are the best fit of the absolute rate theory with ΔH = 62 and 49 kJ mol^{-1} for translocation in POPC and POPC:POPS (9:1), respectively.

translocation of CPZ in the more ordered membranes, containing cholesterol (POPC:Chol:POPS 6:3:1). The results obtained are shown in Figure 6 and indicate that translocation of CPZ between the two leaflets is negligible during the time scale of the titration experiment, γ = 0.5, at both 25 and 37 °C. The inset shows the variation of the global fit χ^2 on the value of γ, indicating that a good global fit is obtained when considering that 40−50% of the lipid is in the outer monolayer of the LUVs. The results impose an upper limit for the rate of translocation in those membranes, which must be equal to or smaller than 4×10^{-4} s^{-1} at both temperatures.

To identify the contributions from cholesterol (reduced membrane fluidity) and POPS (negative charge) in the smaller rate of permeation, we have also characterized the translocation of CPZ in membranes prepared from POPC with 10 mol % POPS. This was first attempted using the uptake and release protocol. However, good release titrations could not be obtained due to the presence of an unexpectedly high heat of dilution and/or heat curves that could not be well described by eqs 1−5 regardless of the accessibility factor considered (results not shown). A tentative interpretation of this observation is related to the opposite charges of POPS and CPZ and the relatively high local concentrations of CPZ required for the release protocol (1 mol %). This may affect the phase behavior of the POPC:POPS bilayer, which shows nonideal mixing even at this small fraction of charged lipid.[61] Changes in the membrane properties upon incubation with CPZ would lead to the occurrence of other processes during dilution in the release protocol, in addition to CPZ equilibration with the aqueous

dx.doi.org/10.1021/ja209917q | J. Am. Chem. Soc. 2012, 134, 4184−4195

phase. In the uptake protocol, no evidence is encountered for unusual processes because the high local concentration of CPZ attained at the beginning of the titration is rapidly decreased as the titration proceeds due to the increase in the concentration of lipid. Effects of CPZ on the phase behavior of charged membranes have been previously observed.[18]

The methodology described above for the case of POPC bilayers was therefore followed to characterize the rate of translocation of CPZ through the POPC:POPS (9:1) bilayers in the temperature range from 25 to 40 °C (Figure 7). The rate of translocation obtained for the charged bilayers in the liquid disordered state is slightly higher than that observed in POPC bilayers, with the best fit values being 1.5×10^{-3} and 1.0×10^{-3} s^{-1}, respectively, at 37 °C and pH = 7.4. (The rate constants for translocation shown are the observed ones corresponding to the average of the rate constants for the neutral and charged species weighted by their relative molar fractions. The expected stabilization of the cationic species at the negatively charged membrane would lead to an increased value of pK_a and a corresponding increase in the fraction of charged CPZ. This effect should have decreased the observed rate constant for translocation.) This result was at first surprising in view of the expected stabilization of the inserted state of the cationic CPZ molecule at the negative surface of the bilayer. The observed increase in the rate of translocation is most likely a result of an overcompensating effect due to the larger free volume in the charged bilayer.[62,63] Increased rates of permeation through negatively charged membranes have been observed by other authors for neutral, zwitterionic, and negatively charged ligands.[64] In that work, the permeation was accelerated by over an order of magnitude for some of the ligands, and the effect on the calculated rate of translocation, eq 9, was even larger for all ligands.

The experiments following the methodology developed in this work for the measurement of the translocation rate constant have been repeated at different temperatures, allowing the calculation of the thermodynamic parameters associated with the formation of the transition state in translocation. The results obtained are shown in Figure 7 and Table 1 and indicate that the slower translocation in POPC bilayers is due to a larger enthalpy variation between the ligand in the inserted and in the transition state (it should be noted that the uncertainty associated with those parameters is very high, due both to the large errors at each temperature and to the small temperature range studied). The entropy variation associated with the formation of the transition state in the translocation process is negative for both membranes, indicating that the bilayer is less disordered when CPZ is located in the bilayer center as compared to CPZ inserted in the leaflets. Similar results have been obtained before for ligands structurally very distinct from the membrane-forming lipids and were interpreted as evidence for the formation of defects in the membrane around the inserted ligand. The effects now observed for CPZ are far more significant than previously obtained for fatty amines and phospholipids,[41,42] because CPZ inserted in the bilayer has the bulky aromatic rings at the carbonyl region,[12] creating a large defect below, in the acyl chain region of the bilayer. Smaller entropies in the translocation transition state have also been observed for bilirubin in POPC bilayers.[65]

When translocation is slower than equilibration between the aqueous and lipid phases, a situation encountered for CPZ in all membrane compositions studied, the permeability coefficient may be calculated from the partition coefficient and translocation rate constant:[42,66−68]

$$P = k_f \lambda K_p \tag{9}$$

where λ is required to convert the ligand concentration from volume to surface units (in the calculations, λ was equal to the radius of the solute, 3.5 Å for the case of CPZ).

The values obtained for the permeability coefficients of CPZ at 25 °C are $P_{POPC} = 1.6 \times 10^{-7}$ cm s^{-1}, $P_{POPC:POPS} = 3.2 \times 10^{-7}$ cm s^{-1}, and $P_{POPC:Chol:POPS} \leq 1 \times 10^{-7}$ cm s^{-1}, and the increase in the temperature to 37 °C leads to a 2-fold increase in the permeability coefficient for both POPC and POPC:POPS membranes. This permeability coefficient is similar to that reported for the hydrophobic ion TPP^+ (tetraphenylphosphonium), $P_{EggPC} \cong 2.0 \times 10^{-8}$ cm s^{-1}.[68] The complete charge delocalization occurring in TPP^+ results in a much faster translocation as compared to CPZ, but this is overcompensated by a much smaller partition coefficient,[68] leading to a similar permeation coefficient.

Permeability coefficients for CPZ across cell monolayers has been measured in vitro, being equal to 2×10^{-8} cm s^{-1}, for confluent MDCK cell monolayers at 37 °C, when measured as the rate of drug entering the receiver container.[69] Significantly larger permeability coefficients are encountered when permeation is evaluated from the rate of drug disappearance from the donor container.[69] However, in this case, it is not transcellular permeation that is being followed but rather the rate of interaction between the drug and the cell monolayer. The permeability coefficient calculated in this work is comparable to that obtained in vitro for MDCK cell monolayers. The faster permeation coefficient obtained for the POPC bilayer is due to the larger fluidity of this model membrane as compared to the apical membrane of MDCK cells that are enriched in sphingomyelin and cholesterol.[70,71]

Effect of CPZ Translocation on the Calculated Partition Coefficient. To analyze the thermograms obtained due to addition of lipid to the ligand, a value must be assumed for the accessibility factor of the lipid (and for both lipid and ligand in the case of the release protocol). In the first section of this work, we have studied the effect of ligand concentration on the observed partition coefficient at 25 °C assuming $\gamma = 0.5$, an approximation that was supported by the positive charge in CPZ and by the global fit to the results following the uptake and release protocols. Given the quantitative characterization of the translocation step using the methodology developed in this work, the value of this parameter at 25 °C may be calculated giving $k_f = 3.9 \times 10^{-4}$ s^{-1}. After the 200 s of each injection, only 8% of the equilibrium value of CPZ in the inner monolayer is attained, further supporting the assumption of slow translocation. It should be noted, however, that equilibrium between the outer and inner monolayer proceeds throughout the titration (~3600 s), and even those small rates of translocation will influence the estimated partition coefficient.

Partial translocation may be included in the calculation of the amount of ligand associated with the bilayer by explicitly considering the outer and the inner leaflets, according to eqs 10−13.

dx.doi.org/10.1021/ja209917q | J. Am. Chem. Soc. 2012, 134, 4184−4195

Table 2. Equilibrium Parameters Obtained for the Partition of CPZ to the Different Membranes Studied Using a Simple Partition Model and after Correction for the Electrostatic Effects[a]

		simple model			corrected for electrostatic interactions		
	T (°C)	K_P^{obs} (10^4)	ΔH (kJ mol^{-1})	$T\Delta S$ (kJ mol^{-1})	K_P (10^4)	ΔH (kJ mol^{-1})	$T\Delta S$ (kJ mol^{-1})
POPC	25	1.3 ± 0.1	−15 ± 2	9	1.5 ± 0.4	−13 ± 1	11
	37	1.4 ± 0.2	−14 ± 1	10	1.4 ± 0.3	−13 ± 1	12
POPC:POPS (9:1)	25	1.5 ± 0.3	−23 ± 3	1	1.0 ± 0.3	−21 ± 3	1
	37	1.3 ± 0.3	−28 ± 6	-4	0.9 ± 0.2	−27 ± 3	−3
POPC:Chol:POPS (6:3:1)	25	0.68 ± 0.03	−5 ± 1	17	0.61 ± 0.03	−4 ± 1	18
	37	0.63 ± 0.08	−14 ± 2	8	0.41 ± 0.04	−12 ± 2	10

[a]The accessibility factor considered was always 0.5 (corresponding to slow CPZ translocation).

The amount of ligand in the outer monolayer at the beginning of the injection ($t = 0$) and at the end of injection i ($t = \delta$) is given by:

$$n^{o}_{CPZ\_L}\Big|_{t=0}(i) = n^{o}_{CPZ\_L}\Big|_{t=\delta}(i-1)\left\{1 + \frac{V(i)}{V_{cell}}\right\}$$

$$n^{o}_{CPZ\_L}\Big|_{t=\delta}(i) = \frac{\left\{n_{CPZ\_T}(i) - n^{i}_{CPZ\_L}\Big|_{t=\delta}(i)\right\}K_P\overline{V}_L[L]^{o}}{1 + K_P\overline{V}_L[L]^{o}} \tag{10}$$

and the amount of ligand in the inner monolayer at the beginning and end of the injection is given by:

$$n^{i}_{CPZ\_L}\Big|_{t=0}(i) = n^{i}_{CPZ\_L}\Big|_{t=\delta}(i-1)\left\{1 + \frac{V(i)}{V_{cell}}\right\}$$

$$n^{i}_{CPZ\_L}\Big|_{t=\delta}(i) = n^{i}_{CPZ\_L}\Big|_{t=\infty}(i) + \{n^{i}_{CPZ\_L}\Big|_{t=0}(i) - n^{i}_{CPZ\_L}\Big|_{t=\infty}(i)\}e^{-\beta\delta}$$

$$\text{with} \quad n^{i}_{CPZ\_L}\Big|_{t=\infty}(i) = n_{CPZ\_T}(i) \times \frac{K_P\overline{V}_L[L]^{i}}{1 + K_P\overline{V}_L[L]^{o} + K_P\overline{V}_L[L]^{i}} \tag{11}$$

where the characteristic rate constant, β, is given by:

$$\beta = k_f\frac{K_P\overline{V}[L]^{i}}{1 + K_P\overline{V}[L]^{o} + K_P\overline{V}[L]^{i}} \tag{12}$$

The moles of ligand that have partitioned to the membrane during injection i (responsible for the heat generated in that titration step) is given by eq 13:

$$\Delta n_{CPZ\_L}(i) = \left\{n^{o}_{CPZ\_L}\Big|_{t=\delta}(i) + n^{i}_{CPZ\_L}\Big|_{t=\delta}(i)\right\} - \left\{n^{o}_{CPZ\_L}\Big|_{t=0}(i) + n^{i}_{CPZ\_L}\Big|_{t=0}(i)\right\} \tag{13}$$

Under the experimental conditions of this work, low ligand concentrations, and 100 nm LUVs, the amount of lipid in the inner and outer leaflet is the same ($[L]^{o} = [L]^{i} = [L]/2$), and the observed partition coefficient may be used in the above equation, being equal for both monolayers. The time between injections was 200 s, and this interval was considered for the calculation of the heat per injection (δ = 200 s).

With the above equations, it is possible to evaluate the effect of the rate of translocation on the calculated parameters. For titrations performed at 25 °C, the inclusion of partial translocation in the model did not significantly affect the values obtained for both K_P^{obs} and ΔH as compared to those obtained without translocation. The values shown in Table 1 (using the observed accessibility factor) and in Table 2 (imposing γ = 0.5) are slightly different from those indicated in the first section of this work because they included all titrations performed that lead to a lipid:CPZ_L ratio above 25 at the first 10 μL injection using $[CPZ]_T$ from 5 to 15 μM and a lipid concentration in the syringe from 5 to 15 mM (over 10 titrations at each temperature), while in the previous section only the titrations with 2.5 and 5 μM CPZ and 5 mM POPC were considered. The less restrictive rule used throughout the work generated a small decrease in the value of K_P^{obs} obtained.

The values obtained for the partition parameters at 37 °C are somewhat more sensitive to the model used due to the occurrence of significant translocation during the titration. Figure 8 shows the best fit of the extreme situations (γ = 0.5 and 1) to a titration profile calculated with the average values of the parameters for CPZ interaction with POPC bilayers at 37 °C ($k_f = 1.0 \times 10^{-3}$ s^{-1}, $K_P^{obs} = 1.0 \times 10^4$, and $\Delta H = -11$ kJ mol^{-1}). The two extreme situations lead exactly to the same shape for the titration curve although with different parameters (K_P^{obs} is reduced to one-half when fast translocation is

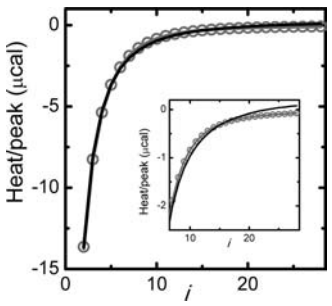

Figure 8. Effect of translocation on the shape of the titration curve. The best fit of a typical titration of 15 μM CPZ with 15 mM POPC at 37 °C is shown in gray (○), and the best fit with very slow and very fast translocation is show in black. The inset shows a closer view of the end of titration to highlight the misfit. The gray curve was obtained with the average values for the parameters (Table 1): $k_f = 1.0 \times 10^{-3}$ s^{-1}, $K_P^{obs} = 1.0 \times 10^4$, and $\Delta H = -11$ kJ mol^{-1}. The best fit of the two extreme conditions has exactly the same shape but different values for the parameters: $k_f = 0$ s^{-1}, $K_P^{obs} = 9.6 \times 10^3$, and $\Delta H = -13$ kJ mol^{-1} (black line) and $k_f = 3.0 \times 10^{-2}$ s^{-1}, $K_P^{obs} = 4.8 \times 10^3$, and $\Delta H = -13$ kJ mol^{-1} (black line).

dx.doi.org/10.1021/ja209917q | J. Am. Chem. Soc. 2012, 134, 4184−4195

considered). There is a clear misfit of the extreme models to the last part of the titration, although it should be noted that when experimental noise is added the distinction between the models could not be done on the basis of a better fit. The deviations observed result from the significant additional heat evolved between 15 and 50 min (injections 5−15) due to translocation of CPZ (with a characteristic time, $\tau_f = 1/k_f$, equal to 17 min) inserted into the outer monolayer in the first injections (over 75% CPZ is associated with the bilayer after injection 6).

In the first section of this work, we report a small but significant increase in the intrinsic partition coefficient of CPZ to POPC membranes at lipid:CPZ molar ratios smaller than 10, Figure 2A. This increase was interpreted as an overcorrection of the electrostatic effects using the Gouy−Chapman theory. The increase observed in K_P may also result from variations in the rate of CPZ translocation at those high local concentrations, an increase in the rate of translocation leading to an accessibility factor larger than the assumed value of 0.5. In fact, the rate of translocation of 50 μM CPZ when titrated with 5 mM POPC (leading to L:CPZ_L equal to 6 after the first 10 μL injection) was sufficiently fast to be measured at 25 °C using the methodology developed in this work and is equal to 2.0×10^{-3} s^{-1} (5 times faster than obtained for smaller local concentrations of CPZ). This result is in agreement with, and gives support to, the qualitative observation of increased lipid scrambling in the presence of relatively high CPZ concentrations.[15−17]

The titrations performed with POPC and with POPC:POPS (9:1), at a lipid to ligand ratio above 25 in the first 10 μL injection, were analyzed with eqs 10−13 taking into account the observed value for the translocation rate constant. The parameters obtained are shown in Table 1.

A small decrease in K_P^{obs} is observed when the temperature is increased from 25 to 37 °C for the association of CPZ with both membranes, in agreement with that predicted for an exothermic process. The thermodynamic parameters obtained indicate that partitioning to the POPC membrane has significant contributions from both enthalpy and entropy, while interaction with the negatively charged membrane is dominated by the enthalpic term.

The value of K_P^{obs} obtained for partitioning to the negatively charged membrane is only slightly higher than that for partitioning to the POPC membrane. This result was unexpected due to the electrostatic interaction between CPZ and the negatively charged membrane, but is in agreement with the reported small increase observed in EggPC:EggPS 9:1 membranes.[30] The thermodynamic parameters obtained in this work allow an interpretation of this result. It can be observed that the relatively small increase in the Gibbs free energy associated with partition of CPZ to the charged membranes is due to a decrease in the entropy contribution that almost balances the more favorable enthalpy contribution observed in the negatively charged membrane. Given that an increase in entropy is expected when CPZ partitions to the membrane, due to the hydrophobic effect, this result points toward a reduction of the entropy of the POPC:POPS membrane upon partition of CPZ. This is in agreement with CPZ perturbation of the (already nonideal) mixing of the two lipids and with the problems encountered with the titrations performed according to the release protocol. From the temperature variation observed for the partition coefficient, the van't Hoff enthalpy may be calculated to be −12 and −5 kJ mol^{-1} for the POPC and POPC:POPS membranes, respectively. The disagreement between the van't Hoff and the calorimetric enthalpy obtained for the charged membrane further supports the occurrence of additional processes in this membrane upon partition of CPZ. The interaction between the head groups of phosphatidyl serine lipids is relatively strong due to the formation of hydrogen bonds, but the electrostatic repulsion between the negatively charged lipids prevents their phase separation in the mixed membranes.[61] Changes in the electrostatic potential of the bilayer may affect their phase behavior. On the basis of the results obtained, we speculate that the cationic ligand CPZ induces POPS clustering (and eventually phase separation) in the POPC:POPS 9:1 membrane.

The comparison between the affinities of CPZ for both membranes is more easily done after deconvolution of the observed partition coefficient into the electrostatic and hydrophobic contributions. This may be done through the computation of the intrinsic partition coefficient (K_P), via eqs 4 and 5, and will be performed in the next section together with the results obtained for the additional membrane composition studied (POPC:Chol:POPS 6:3:1).

Effect of Lipid Composition in the Interaction of CPZ with Lipid Bilayers. The parameters obtained for the interaction of CPZ with all membranes studied are summarized in Table 2. The best fit of the simple model (eqs 1−3) provides the observed partition coefficient, K_P^{obs}, and enthalpy variation allowing the comparison between the different membranes in terms of the effective amount of CPZ that associates with them at the experimental conditions used (lipid:CPZ_L ≥ 25 at the first titration step). In this model, the interaction is interpreted globally, without distinction between the contributions from hydrophobic and electrostatic interactions. To compare charged and neutral membranes, it is preferable to separate the two types of interactions, and this may be done through the calculation of the intrinsic partition coefficient, K_P, where the electrostatic interactions have been taken into account explicitly using the Gouy−Chapman theory (eqs 4 and 5). It is not possible to consider partial translocation (according to the model developed in this work) and correction for electrostatic effects due to the different values of the effective partition coefficient and rate of translocation that would be required for the inner and outer leaflet. The required model to account for this situation is too complex, and with too many unknown variables, to be of practical utility. For all membranes and temperatures studied, the approximation of slow translocation was always closer to the observed behavior, and therefore the parameters shown in Table 2 after correction for the electrostatic effects have all been calculated assuming $\gamma = 0.5$.

The comparison of the partition coefficient obtained from the two models for CPZ interaction with the zwitterionic POPC membrane indicates that even with the small concentrations of CPZ used (5−15 μM), the charge imposed by CPZ in the membrane is still significant. The POPC:CPZ_L ratios varied from ∼30 to over 100 at the end of the titration being typically around 50 at 50% ligand titrated. At this local concentration of CPZ, the calculated surface potential is 9 mV, originating a reduction in the observed partition coefficient of nearly 20%, according to eq 4.

The electrostatic contributions in the case of membranes containing POPS are of two types: (i) electrostatic attraction between the negatively charged membrane and the cationic CPZ, and (ii) change in the membrane charge due to the presence of CPZ. The two effects have been taken into account in the model by using both CPZ and POPS charges in eq 5. In the absence of CPZ, the calculated surface potential of the

dx.doi.org/10.1021/ja209917q | J. Am. Chem. Soc. 2012, 134, 4184−4195

membranes with 10% POPS is equal to −26 mV, and for the typical ratios at 50% titration the surface potential is reduced to −21 mV, both conditions leading to an attractive electrostatic interaction between CPZ and the membrane surface. The ζ potentials of POPC:POPS 9:1 liposomes with and without CPZ were also measured and were in qualitative agreement with those calculated for the surface potential using the Gouy−Chapman theory (see the Supporting Information). The exclusion of this electrostatic interaction leads to a reduction in the calculated intrinsic partition coefficient (K_P) that is smaller than the observed partition (K_P^{obs}) for those negatively charged membranes (Table 2).

The comparison of the intrinsic partition coefficients obtained for POPC and POPC:POPS indicates that the hydrophobic contribution to solvation of CPZ by the lipid bilayer is smaller for the charged membrane. This may reflect the more superficial location proposed for CPZ when associated with negatively charged membranes.[14]

The introduction of cholesterol in the membrane leads to a reduction in both the partition coefficient and the interaction enthalpy. In fact, the characterization of CPZ partition to POPC:Chol 7:3 membranes by ITC was attempted, but the heat change involved was too small. This is in agreement with the results obtained for the interaction of other ligands with POPC:Chol membranes[72,73] and highlights the poor solvation properties of those ordered membranes. The addition of POPS to the bilayer increases the heat change involved in the interaction, due to the electrostatic interaction between CPZ and the negatively charged membrane, and allows its characterization by ITC. The comparison between the results obtained with POPC:POPS and POPC:Chol:POPS indicates a decrease in the partition coefficient to nearly one-half due to the addition of cholesterol. This result is in excellent agreement with published results for the effect of 30% cholesterol in EggPC membranes.[26] The temperature variation of the interaction enthalpy with membranes containing 10% POPS and 30% cholesterol is even more accentuated than that observed for POPC:POPS 9:1. This result reinforces the interpretation that, at low temperatures, POPS and POPC do not mix well in the presence of CPZ and indicates that this effect is accentuated by the presence of cholesterol in the membrane.

CONCLUSIONS

In this work, we have developed methodology, which allows the quantitative characterization of the translocation of ligands through lipid bilayers using the ITC technique. This complements the available protocols for describing qualitatively this process.[31] The rate of translocation of CPZ through the membranes in the liquid disorder phase has been measured: 3.9×10^{-4} and 6.6×10^{-4} s^{-1} for POPC and POPC:POPS 9:1, respectively, at 25 °C and nearly twice as large at 37 °C. Together with the partition coefficient measured, this allows the calculation of the permeability coefficient, which is equal to 2.0×10^{-7} cm s^{-1} for POPC, 3.9×10^{-7} cm s^{-1} for POPC:POPS 9:1, and smaller than 5.0×10^{-8} cm s^{-1} for POPC:Chol:POPS 6:3:1 membranes at 37 °C. The values obtained are similar to that reported for other hydrophobic cations[68] and to that observed in vitro for permeation through MDCK cell monolayers.[69] Local concentrations of CPZ in the POPC membrane above 10 mol % lead to an increase in the rate of CPZ translocation, which may be explained by the increased lipid scrambling[15−17] and may be of relevance to the observed suppression of multi drug resistance[22−24] by high CPZ concentrations.

The introduction of negative charge in the membrane leads only to a small increase in the observed partition coefficient (1.3×10^4 and 1.5×10^4 for POPC and POPC:POPS 9:1, respectively). This is due to the much smaller entropy variation observed for partition to the negatively charged membrane that almost counterbalance the more favorable enthalpy variation due to the electrostatic interaction between CPZ and the membrane. This and other unexpected observations and results obtained for the membranes containing POPS suggest that CPZ may be inducing some changes in the phase behavior of the membranes, eventually leading to POPS clustering or phase separation, even at the low local concentrations used in this work.

The addition of cholesterol to the POPC bilayer reduces the affinity of CPZ to the membrane, which becomes essentially driven by entropy and therefore inaccessible by ITC. The addition of POPS to the membrane increases the interaction enthalpy and allowed the characterization of the partition of CPZ to POPC:Chol:POPS 6:3:1 membranes. The partition coefficient obtained was reduced by 50% due to the presence of cholesterol and the consequent ordering of the lipid bilayer. The translocation of CPZ through those membranes was too slow to be measured using the available methodology, and only an upper limit may be established, $k_f \leq 4 \times 10^{-4}$ s^{-1}.

ASSOCIATED CONTENT

Supporting Information

Characterization of LUVs size, ζ potential, and multilamellarity. This material is available free of charge via the Internet at http://pubs.acs.org.

AUTHOR INFORMATION

Corresponding Author

mmoreno@ci.uc.pt

Notes

The authors declare no competing financial interest.

ACKNOWLEDGMENTS

This work was supported by research grants from the Portuguese Ministry for Science and Higher Education through FCT, via the PTDC program cofinanced by the European Union (Project 64565), and from the Spanish Ministry of Science and Innovation (BFU2010-19451). P.T.M. and R.M.S.C. acknowledge FCT for their Ph.D. fellowships SFRH/BD/38951/2007 and SFRH/BD/45453/2008, respectively.

REFERENCES

(1) Kramer, S. D.; Lombardi, D.; Primorac, A.; Thomae, A. V.; Wunderli-Allenspach, H. *Chem. Biodiversity* **2009**, *6*, 1900−1916.

(2) Sawada, G. A.; Barsuhn, C. L.; Lutzke, B. S.; Houghton, M. E.; Padbury, G. E.; Ho, N. F. H.; Raub, T. J. *J. Pharmacol. Exp. Ther.* **1999**, *288*, 1317−1326.

(3) Jing, P.; Rodgers, P. J.; Amemiya, S. *J. Am. Chem. Soc.* **2009**, *131*, 2290−2296.

(4) Attwood, D. *Adv. Colloid Interface Sci.* **1995**, *55*, 271−303.

(5) Kitamura, K.; Takenaka, M.; Yoshida, S.; Ito, M.; Nakamura, Y.; Hozumi, K. *Anal. Chim. Acta* **1991**, *242*, 131−135.

(6) Wajnberg, E.; Tabak, M.; Nussenzveig, P. A.; Lopes, C. M. B.; Louro, S. R. W. *Biochim. Biophys. Acta* **1988**, *944*, 185−190.

(7) Attwood, D.; Boitard, E.; Dubes, J. P.; Tachoire, H. *J. Phys. Chem.* **1992**, *96*, 11018−11021.

(8) Attwood, D.; Waigh, R.; Blundell, R.; Bloor, D.; Thevand, A.; Boitard, E.; Dubes, J. P.; Tachoire, H. *Magn. Reson. Chem.* **1994**, *32*, 468−472.
(9) Luxnat, M.; Galla, H. J. *Biochim. Biophys. Acta* **1986**, *856*, 274−282.
(10) Welti, R.; Mullikin, L. J.; Yoshimura, T.; Helmkamp, G. M. *Biochemistry* **1984**, *23*, 6086−6091.
(11) Kitamura, K.; Goto, T.; Kitade, T. *Talanta* **1998**, *46*, 1433−1438.
(12) Kuroda, Y.; Kitamura, K. *J. Am. Chem. Soc.* **1984**, *106*, 1−6.
(13) Kitamura, K.; Takegami, S.; Kobayashi, T.; Makihara, K.; Kotani, C.; Kitade, T.; Moriguchi, M.; Inoue, Y.; Hashimoto, T.; Takeuchi, M. *Biochim. Biophys. Acta, Biomembr.* **2004**, *1661*, 61−67.
(14) Agasosler, A. V.; Tungodden, L. M.; Cejka, D.; Bakstad, E.; Sydnes, L. K.; Holmsen, H. *Biochem. Pharmacol.* **2001**, *61*, 817−825.
(15) Ahyayauch, H.; Bennouna, M.; Alonso, A.; Goni, F. M. *Langmuir* **2010**, *26*, 7307−7313.
(16) Rosso, J.; Zachowski, A.; Devaux, P. F. *Biochim. Biophys. Acta* **1988**, *942*, 271−279.
(17) Schrier, S. L.; Zachowski, A.; Devaux, P. F. *Blood* **1992**, *79*, 782−786.
(18) Jutila, A.; Soderlund, T.; Pakkanen, A. L.; Huttunen, M.; Kinnunen, P. K. J. *Chem. Phys. Lipids* **2001**, *112*, 151−163.
(19) Hidalgo, A. A.; Caetano, W.; Tabak, M.; Oliveira, O. N. *Biophys. Chem.* **2004**, *109*, 85−104.
(20) Hanpft, R.; Mohr, K. *Biochim. Biophys. Acta* **1985**, *814*, 156−162.
(21) Hornby, A. P.; Cullis, P. R. *Biochim. Biophys. Acta* **1981**, *647*, 285−292.
(22) Wadkins, R. M.; Houghton, P. J. *Biochim. Biophys. Acta* **1993**, *1153*, 225−236.
(23) Michalak, K.; Wesolowska, O.; Motohashi, N.; Molnar, J.; Hendrich, A. B. *Curr. Drug Targets* **2006**, *7*, 1095−1105.
(24) Hendrich, A. B.; Wesolowska, O.; Pola, A.; Motohashi, N.; Molnar, J.; Michalak, K. *Mol. Membr. Biol.* **2003**, *20*, 53−60.
(25) Kitamura, K.; Imayoshi, N.; Goto, T.; Shiro, H.; Mano, T.; Nakai, Y. *Anal. Chim. Acta* **1995**, *304*, 101−106.
(26) Takegami, S.; Kitamura, K.; Kitade, T.; Hasegawa, K.; Nishihira, A. *J. Colloid Interface Sci.* **1999**, *220*, 81−87.
(27) Takegami, S.; Kitamura, K.; Kitade, T.; Kitagawa, A.; Kawamura, K. *Chem. Pharm. Bull.* **2003**, *51*, 1056−1059.
(28) Moreno, M. J.; Bastos, M.; Velazquez-Campoy, A. *Anal. Biochem.* **2010**, *399*, 44−47.
(29) Tan, A. M.; Ziegler, A.; Steinbauer, B.; Seelig, J. *Biophys. J.* **2002**, *83*, 1547−1556.
(30) Takegami, S.; Kitamura, K.; Kitade, T.; Takashima, M.; Ito, M.; Nakagawa, E.; Sone, M.; Sumitani, R.; Yasuda, Y. *Chem. Pharm. Bull.* **2005**, *53*, 147−150.
(31) Tsamaloukas, A. D.; Keller, S.; Heerklotz, H. *Nat. Protoc.* **2007**, *2*, 695−704.
(32) Heerklotz, H. *J. Phys.: Condens. Matter* **2004**, *16*, R441−R467.
(33) Heerklotz, H. H.; Binder, H.; Epand, R. M. *Biophys. J.* **1999**, *76*, 2606−2613.
(34) Andreas, M.; Peter, P. *ChemPhysChem* **2009**, *10*, 1405−1414.
(35) Hope, M. J.; Bally, M. B.; Webb, G.; Cullis, P. R. *Biochim. Biophys. Acta* **1985**, *812*, 55−65.
(36) Bartlett, G. R. *J. Biol. Chem.* **1959**, *234*, 466−468.
(37) Taylor, R. P.; Broccoli, A. V.; Grisham, C. M. *J. Chem. Educ.* **1978**, *55*, 63−64.
(38) Jones, M. N. *Adv. Colloid Interface Sci.* **1995**, *54*, 93−128.
(39) Ozbek, H. Viscosity of Aqueous Sodium Chloride Solutions from 0−150 °C. Accessed on 21/12/2011, Lawrence Berkeley National Laboratory, LBNL paper LBL-5931; http://escholarship.org/uc/item/3jp6n2bf.
(40) Nortemann, K.; Hilland, J.; Kaatze, U. *J. Phys. Chem. A* **1997**, *101*, 6864−6869.
(41) Cardoso, R. M. S.; Martins, P. A. T.; Gomes, F.; Doktorovova, S.; Vaz, W. L. C.; Moreno, M. J. *J. Phys. Chem. B* **2011**, *115*, 10098−10108.
(42) Moreno, M. J.; Estronca, L. M. B. B.; Vaz, W. L. C. *Biophys. J.* **2006**, *91*, 873−881.
(43) Freire, E.; Schon, A.; Velazquez-Campoy, A. *Methods in Enzymology: Biothermodynamics*; 2009; Vol. *455*, pp 127−155.
(44) Velazquez-Campoy, A.; Freire, E. *Nat. Protoc.* **2006**, *1*, 186−191.
(45) Velazquez-Campoy, A.; Freire, E. *Biophys. Chem.* **2005**, *115*, 115−124.
(46) Wiener, M. C.; White, S. H. *Biophys. J.* **1992**, *61*, 428−433.
(47) Krivanek, R.; Okoro, L.; Winter, R. *Biophys. J.* **2008**, *94*, 3538−3548.
(48) Keller, S.; Heerklotz, H.; Jahnke, N.; Blume, A. *Biophys. J.* **2006**, *90*, 4509−4521.
(49) do Canto, A.; Carvalho, A. J. P.; Ramalho, J.; Loura, L. M. S. *Biophys. Chem.* **2011**, *159*, 275−286.
(50) Sampaio, J. L.; Moreno, M. J.; Vaz, W. L. C. *Biophys. J.* **2005**, *88*, 4064−4071.
(51) Matos, C.; Lima, J. L. C.; Reis, S.; Lopes, A.; Bastos, M. *Biophys. J.* **2004**, *86*, 946−954.
(52) Torrie, G. M.; Valleau, J. P. *J. Phys. Chem.* **1982**, *86*, 3251−3257.
(53) Murray, D.; Arbuzova, A.; Hangyas-Mihalyne, G.; Gambhir, A.; Ben-Tal, N.; Honig, B.; McLaughlin, S. *Biophys. J.* **1999**, *77*, 3176−3188.
(54) Shapovalov, V. L.; Brezesinski, G. *J. Phys. Chem. B* **2006**, *110*, 10032−10040.
(55) Heerklotz, H. *Q. Rev. Biophys.* **2008**, *41*, 205−264.
(56) Tatulian, S. A. *Eur. J. Biochem.* **1987**, *170*, 413−420.
(57) Beschiaschvili, G.; Seelig, J. *Biochemistry* **1992**, *31*, 10044−10053.
(58) Thomae, A. V.; Wunderli-Allenspach, H.; Kramer, S. D. *Biophys. J.* **2005**, *89*, 1802−1811.
(59) Chakrabarti, A. C. *Amino Acids* **1994**, *6*, 213−229.
(60) Abraham, M. H. *J. Pharm. Sci.* **2011**, *100*, 1690−1701.
(61) Huang, J. Y.; Swanson, J. E.; Dibble, A. R. G.; Hinderliter, A. K.; Feigenson, G. W. *Biophys. J.* **1993**, *64*, 413−425.
(62) Manuel, M.; Martins, J. *Chem. Phys. Lipids* **2008**, *154*, 79−86.
(63) Luna, C.; Stroka, K. M.; Bermudez, H.; Aranda-Espinoza, H. *Colloids Surf., B* **2011**, *85*, 293−300.
(64) Thomae, A. V.; Koch, T.; Panse, C.; Wunderli-Allenspach, H.; Kramer, S. D. *Pharm. Res.* **2007**, *24*, 1457−1472.
(65) Zucker, S. D.; Goessling, W.; Hoppin, A. G. *J. Biol. Chem.* **1999**, *274*, 10852−10862.
(66) Laidler, K. J.; Shuler, K. E. *J. Chem. Phys.* **1949**, *17*, 851−855.
(67) Zwolinski, B. J.; Eyring, H.; Reese, C. E. *J. Phys. Colloid Chem.* **1949**, *53*, 1426−1453.
(68) Flewelling, R. F.; Hubbell, W. L. *Biophys. J.* **1986**, *49*, 531−540.
(69) Sawada, G. A.; Ho, N. F. H.; Williams, L. R.; Barsuhn, C. L.; Raub, T. J. *Pharm. Res.* **1994**, *11*, 665−673.
(70) Simons, K.; Fuller, S. D. *Annu. Rev. Cell Biol.* **1985**, *1*, 243−288.
(71) Simons, K.; Vaz, W. L. C. *Annu. Rev. Biophys. Biomol. Struct.* **2004**, *33*, 269−295.
(72) McIntosh, T. J.; Vidal, A.; Simon, S. A. *Biochem. Soc. Trans.* **2001**, *29*, 594−598.
(73) Estronca, L. M. B. B.; Moreno, M. J.; Vaz, W. L. C. *Biophys. J.* **2007**, *93*, 4244−4253.